Harada et al., http://www.jcb.org/cgi/content/full/jcb.201308029/DC1

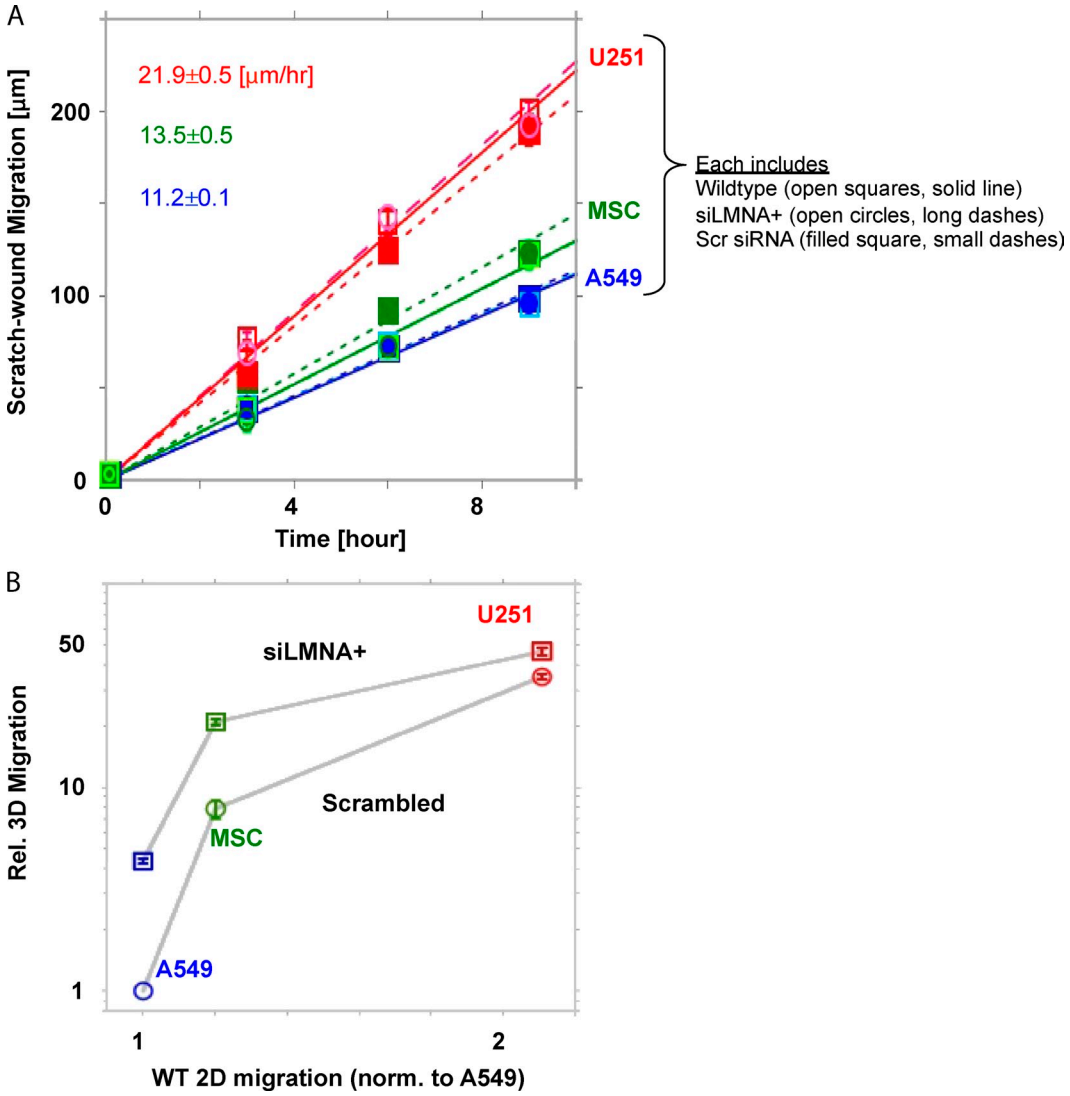

Figure S1. **Moderate changes in lamin-A do not affect 2D migration, but 2D migration always correlates positively with 3D migration.** (A) Scratch-wound assay for lamin-A knockdown (open circles) as well as wild-type (open squares) and scrambled siRNA-treated (filled squares) cells ($n > 3$; ±SEM). (B) Relative migration efficacy of siLMNA$^+$ and control siRNA-treated cells is plotted against relative migration velocity on surface measured in Fig. S2 A for A549, MSC, and U251. Control siRNA-treated A549 is set as 1 for both axes.

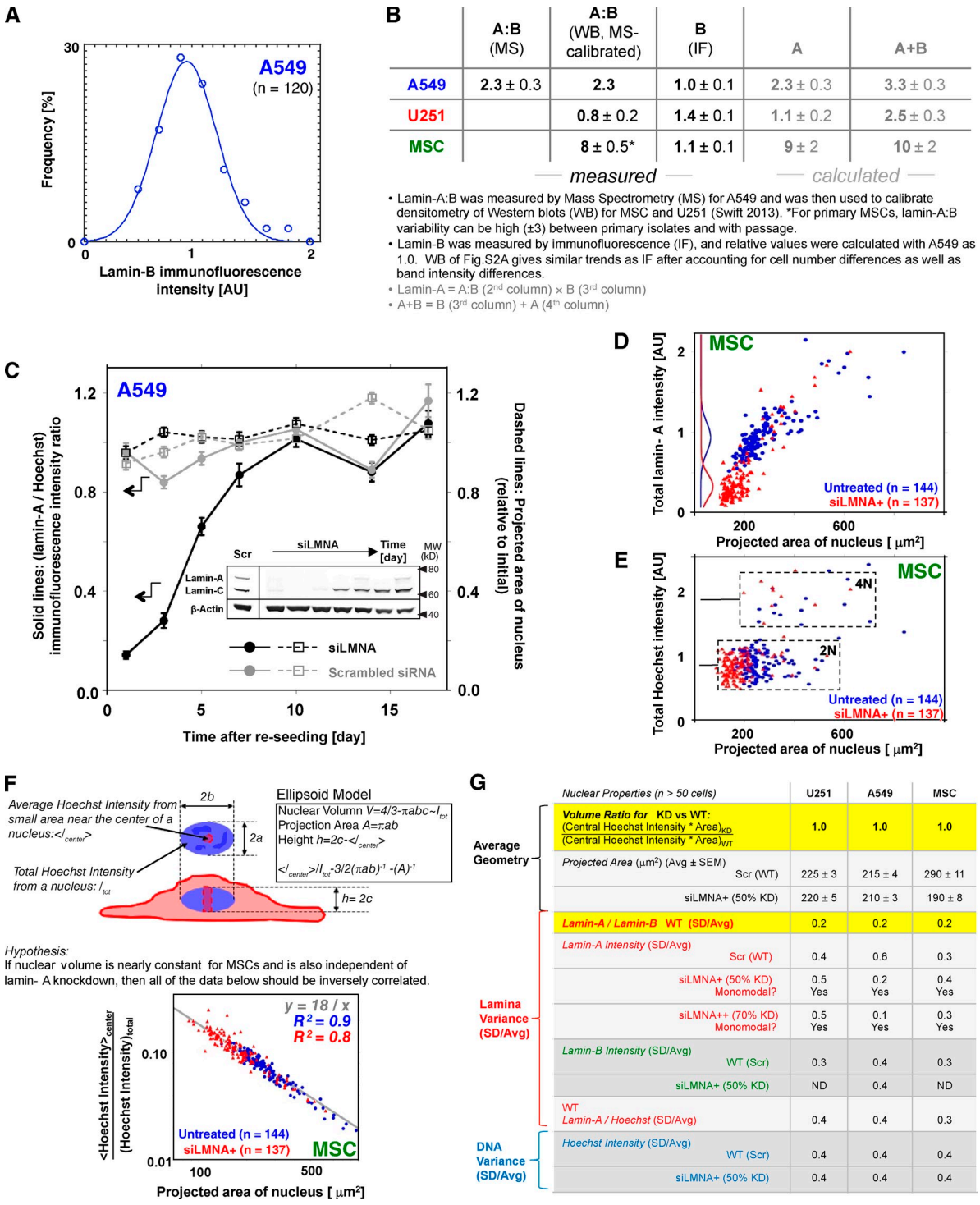

Figure S2. **Isoform ratios can be calibrated by mass spectrometry for comparisons between cell types, and single cell measurements of nuclear properties reveal no change in nuclear volume with knockdown.** (A) Histogram of in vitro immunofluorescence for lamin-B (n = 120). (B) Table summarizing lamin-A:B, B, A, and (A+B) values for A549, MSC, and U251 cells. Calculations used for obtaining values appearing in inset bar graphs of Fig. 1 C are explained below the table. (C) Changes in normalized lamin-A expression (filled circles) and projected nuclear area (open circles) after either siLMNA or scrambled siRNA treatment were monitored over 17 d (n > 50; ±SEM). Inset is immunoblot image of A549 cells treated with either scrambled siRNA (Scr) or siLMNA. For siLMNA treatment conditions, A549 cells were collected for Western blot measurements at different time points corresponding to the ones on the main plot. The bands correspond to lamin-A, lamin-C, and β-actin from top to bottom. (D and E) Quantitative immunofluorescence of lamins and Hoechst analysis of single cells was done after lamin-A knockdown (siLMNA$^+$) versus scrambled (Scr). Data for MSCs are shown (n > 130). (F) Nuclear volume analysis based on nuclear area and averaged Hoechst intensity in a small area at the center of the nucleus, proportional to nuclear height. (G) Table of nuclear properties, with the ratio of nuclear volumes highlighted together with the small coefficient of variation in the lamin-A:B ratio. For most properties measured, the wild-type (or Scr) and knockdown cells did not differ.

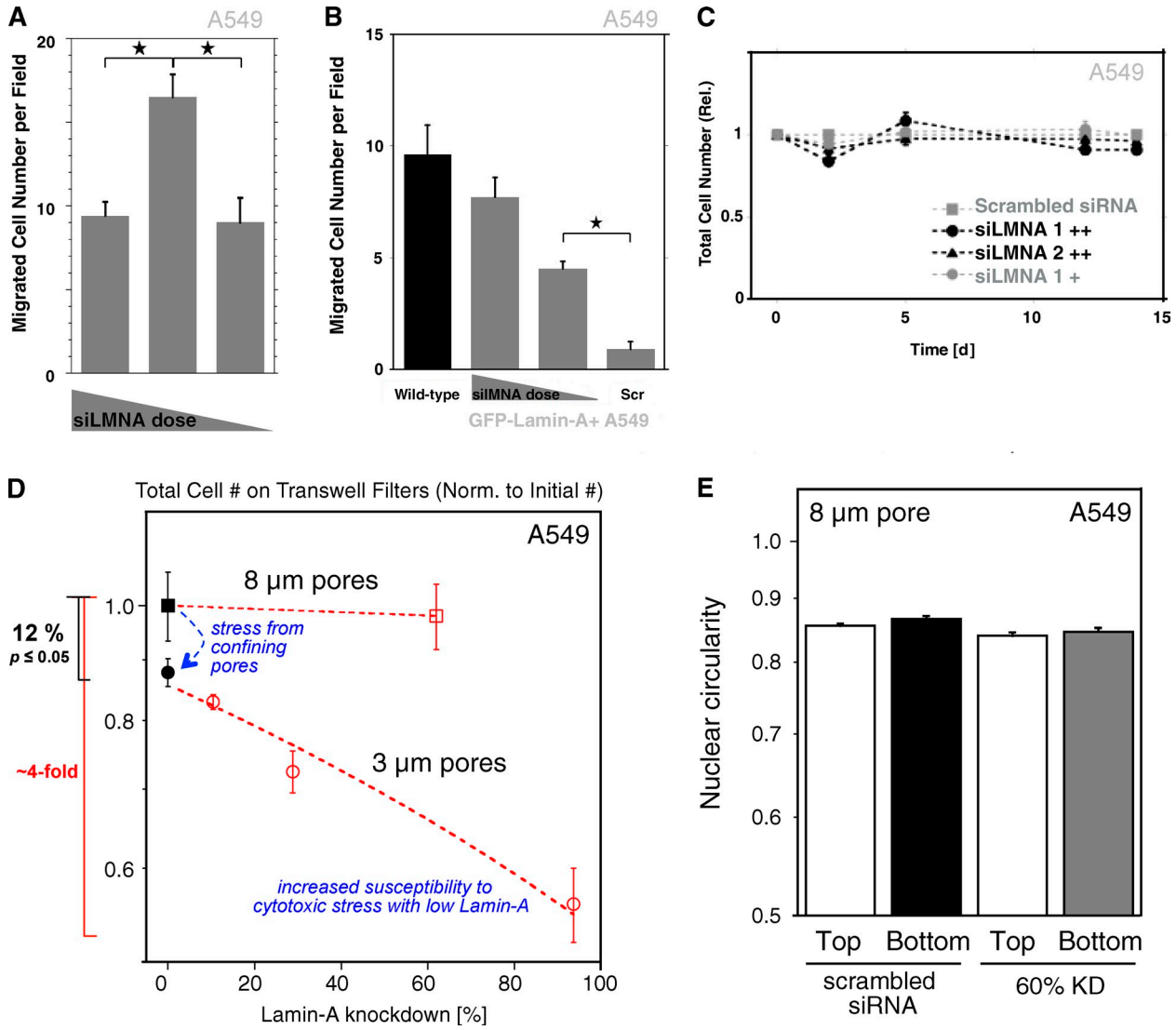

Figure S3. **siLMNAs with distinct targets consistently increase 3D migration without affecting viability in 2D or else viability and nuclear shape after large pore migration, but cell numbers are reduced with small pores and with knockdown.** (A) Non-linear dose dependence of A549 migration (3-µm pores) with siLMNA2 (n = 10; ±SEM; star, $P < 0.01$). (B) Recovery of suppressed migration capacity in GFP-lamin-A–overexpressing A549 cells by partial lamin-A knockdown (n = 10; ±SEM; star, $P < 0.01$). (C) Cell proliferation assay of siLMNA-treated cells, showing relative cell viability against scrambled siRNA control on the same time points (n = 2; ±SEM). (D) Total cell numbers on both sides of Transwell filters after normalization to control, with the same initial number of cells seeded for all doses of Scr or siLMNA (n = 3; ±SEM; star, $P < 0.05$). (E) Negligible influence of migration through 8-µm pore filter on nuclear circularity, irrespective of lamin-A knockdown (n = 3 experiments with > 160 cells each; ±SEM).

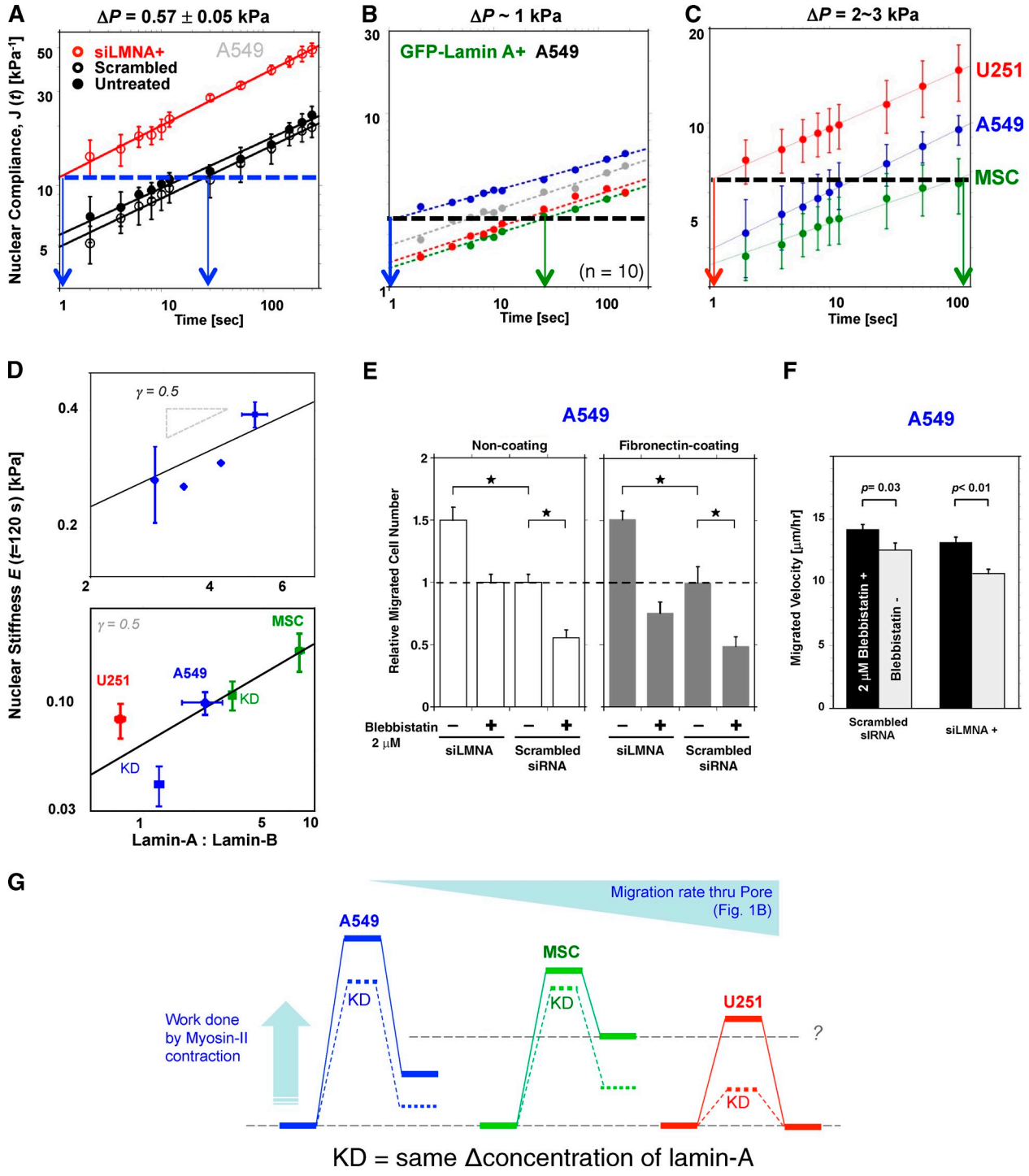

Figure S4. **Micropipette aspiration reveals lamin-A prolongs relaxation times and effectively stiffens nuclei, whereas lamin-B confers elasticity and shortens relaxation times and myosin-II drives migration through small pores.** (A) A549 nuclear compliance change with time under constant pressure (~0.5 kPa) with a power law fit for siLMNA$^+$ and control cells (n = 4; ±SEM). (B) Nuclear compliance of GFP-lamin-A–overexpressing A549 cells. (C) Nuclear compliance change with time of A549, MSC, and U251 cells under 2–3 kPa pressure ($n \geq 4$; ±SEM). (D) Apparent nuclear stiffness obtained with micropipette aspiration for GFP-lamin-A–overexpressing A549 cells (top) and the three cell lines (bottom, $n \geq 4$; ±SEM). (E) Transwell migration assay after treatment with myosin-II inhibitor blebbistatin. A549 cells with lamin-A knockdown were induced to migrate through 3-μm pores in the presence of 2 μM blebbistatin with no coating (left) or fibronectin coating (right). Stars represent statistically significant difference ($n \geq 18$; ±SEM; star, $P < 0.05$). (F) Effect of blebbistatin (2 μM) treatment of 2D migration velocity of A549 cells, either treated with siLMNA$^+$ or control siRNA (n = 3; ±SEM). (G) Schematic of nuclear barrier for each cell type (related to Fig. 2 F) and the effect of similar mass of lamin-A knockdown. Work done by myosin-II overcomes the activation barrier that decreases with lamin-A knockdown in each on cell type. Because nuclei in U251 cells fully recover their shape after migration, the energy difference between nuclei on top and bottom is nearly zero and is unaffected by knockdown. In contrast, because nuclei in MSCs maintain highly distorted nuclei on the bottom compared with the top (see Fig. 2), it seems likely that energy remains stored in the lamin-B network (on the time scale of the measurements) and that knockdown decreases this energy difference. A549 cells are an intermediate case.

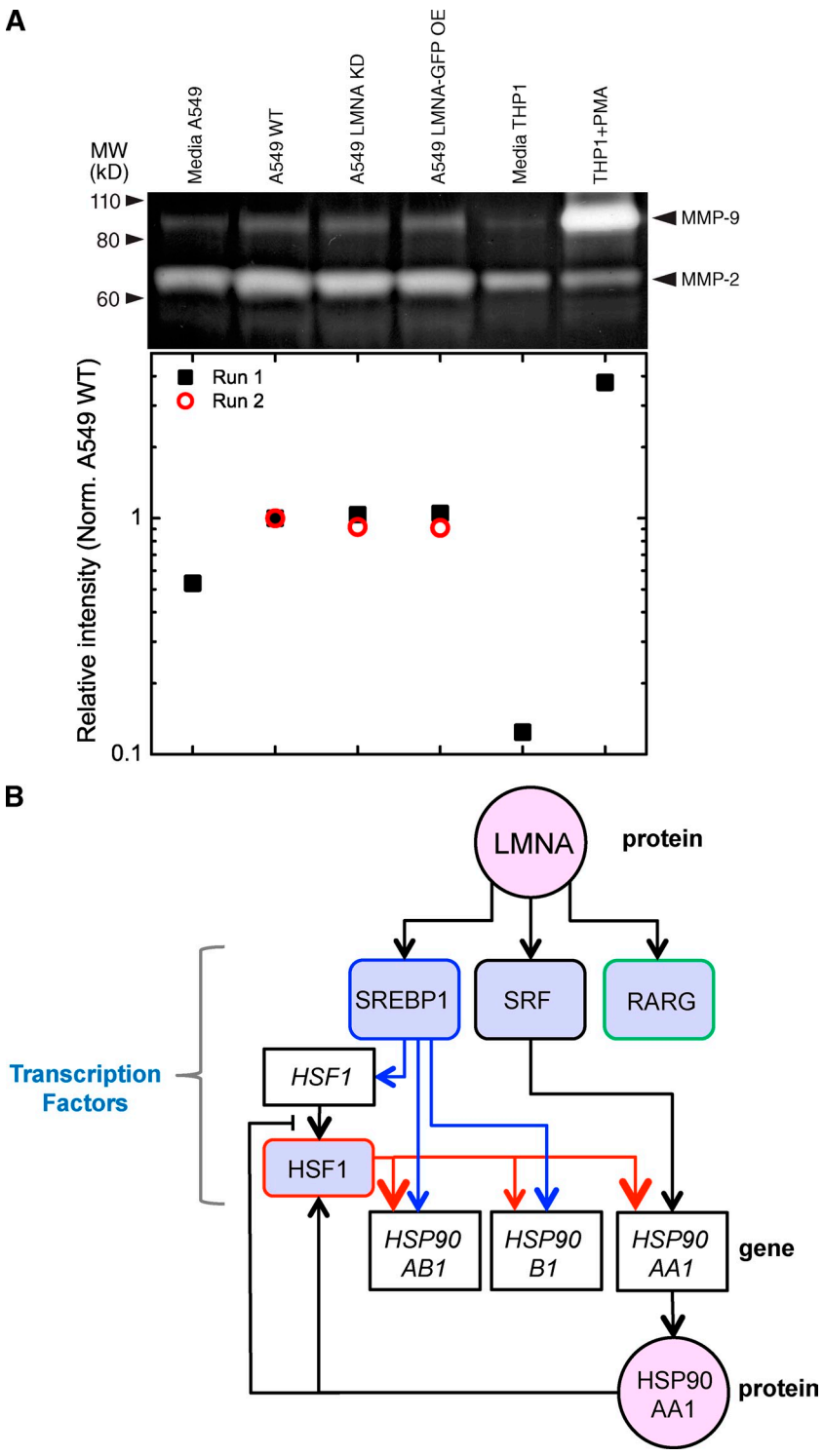

Figure S5. **Lamin-A levels do not affect MMPs as determined by zymogram assay, whereas deep knockdown of lamin-A suppresses HSP90 consistent with lamin-A regulation of transcription factors impacting the HSP90 pathway.** (A) Zymogram assay of A549 culture media without cells, with wild-type A549s (WT), lamin-A knockdown A549s (KD), and A549s with lamin-A overexpression (OE). As a positive control, we also include culture media of THP1 macrophages treated with PMA, which is known to produce MMP-9. All samples were acquired after 5 d of culture. Densitometry was performed using ImageJ. (B) Moderate knockdown of *LMNA* showed no effect on any HSP90 transcripts, but does impact the SRF (Ho et al., 2013; Swift et al., 2013b) and RARG (Swift et al., 2013b), and lamin-A is already known to interact with SREBF1 (Lloyd et al., 2002). Chromatin immunoprecipitation (Rosenbloom et al., 2013) has revealed SREBP1 binds weakly to the promoter of HSF1 (cluster score: 58 on a scale of 1,000) as well as the promoter regions of constitutive HSP90AB1 (cluster score: 161) and HSP90B1 (cluster score: 437). SRF interacts weakly with inducible HSP90AA1 (cluster score: 106). HSF1 is a master regulator of all HSP90s with measurable interactions with all promoters (AB1, B1, and AA1 have respective cluster scores of 973, 243, and 1,000). Feedback is provided by HSF1 interactions with inducible HSP90AA1 (Zou et al., 1998). Thin arrows indicate low cluster scores.

References

Ho, C.Y., D.E. Jaalouk, M.K. Vartiainen, and J. Lammerding. 2013. Lamin A/C and emerin regulate MKL1-SRF activity by modulating actin dynamics. *Nature*. 497:507–511. http://dx.doi.org/10.1038/nature12105

Lloyd, D.J., R.C. Trembath, and S. Shackleton. 2002. A novel interaction between lamin A and SREBP1: implications for partial lipodystrophy and other laminopathies. *Hum. Mol. Genet.* 11:769–777. http://dx.doi.org/10.1093/hmg/11.7.769

Rosenbloom, K.R., C.A. Sloan, V.S. Malladi, T.R. Dreszer, K. Learned, V.M. Kirkup, M.C. Wong, M. Maddren, R.H. Fang, S.G. Heitner, et al. 2013. ENCODE data in the UCSC Genome Browser: year 5 update. *Nucleic Acids Res.* 41(D1, Database issue):D56–D63. http://dx.doi.org/10.1093/nar/gks1172

Swift, J., I.L. Ivanovska, A. Buxboim, T. Harada, P.C.D.P. Dingal, J. Pinter, J.D. Pajerowski, K.R. Spinler, J.-W. Shin, M. Tewari, et al. 2013b. Nuclear lamin-A scales with tissue stiffness and enhances matrix-directed differentiation. *Science*. 341:1240104. http://dx.doi.org/10.1126/science.1240104

Zou, J.Y., Y.L. Guo, T. Guettouche, D.F. Smith, and R. Voellmy. 1998. Repression of heat shock transcription factor HSF1 activation by HSP90 (HSP90 complex) that forms a stress-sensitive complex with HSF1. *Cell*. 94:471–480. http://dx.doi.org/10.1016/S0092-8674(00)81588-3